Mapping seasonal and interannual Non-Structural Carbohydrate variation to drought-resistance strategies in eastern Amazon tree species

Mauro Brum[1], Scott Saleska[1], Luciana F Alves[2], Deliane Penha[3], Valeriy Ivanov[4], Natalia Restrepo-Coupe[1], Loren Albert[5], Raimundo Oliveira-Junior[6], José Mauro Moura[3], Sarah Mião[7], Caroline Signori-Müller[7], Neill Prohaska[1], Luiz Aragão[8], and Rafael Oliveira[9]

[1]The University of Arizona Department of Ecology and Evolutionary Biology
[2]University of California Los Angeles
[3]Universidade Federal do Oeste do Para
[4]University of Michigan
[5]Brown University
[6]EMBRAPA Amazônia Oriental
[7]UNICAMP IB
[8]Instituto Nacional de Pesquisas Espaciais
[9]University of Campinas

March 24, 2021

Abstract

Carbon allocation to non-structural carbohydrates (NSC) is essential for plant metabolism playing an important role in tree responses to drought. It is still unclear if and how interspecific hydraulic trait variation modulates NSC concentration dynamics in different plant organs, particularly in tropical tree species. We investigated whether drought-resistance strategies (inferred from hydraulic traits) explain seasonal and interannual NSC dynamics in leaves, branches, trunks, and roots in seasonal eastern Amazon tree species in Brazil. We measured NSC concentration in eight abundant species during three years, including the end of the wet and dry seasons of the typical regular years (2013-2014) and the extreme drought induced by El Niño–Southern Oscillation in 2015 (ENSO). Organs have an important contribution to explain the starch (ST), soluble sugar (SS), and NSC variance among trees. We showed seasonal and year-to-year homeostasis in ST and SS concentrations in a majority of organs during 2013 and 2014, but SS increased in all organs during the extreme ENSO drought, while the ST concentration did not. The increase in SS concentration was more evident in woody organs from species with intermediate and tolerant drought strategies. The drought-tolerant species maintain higher root starch concentrations and mobilize more SS during extreme drought.

Introduction

Understanding how functional trait diversity modulates ecosystem processes is crucial for improving predictions of tropical forest responses to climate change (Sterck, Markesteijn, Schieving & Poorter 2011; Allen, Breshears & McDowell 2015; Barros *et al.* 2019). Most of evergreen Amazon forests annually experience a distinct dry season, taken to be the period when monthly precipitation falls below 100 mm (Sombroek 2001, Restrepo-Coupe *et al* . 2016). Further, prolonged water stress periods caused by El Niño Southern Oscillation (ENSO) events are also becoming more frequent in this region (Marengo, Tomasella, Alves, Soares & Rodriguez 2011; Jiménez-Muñoz *et al.*2016; Brum *et al* . 2018), inducing changes in forest metabolism and nutrient cycling (Doughty *et al* . 2015; Hartmann *et al* . 2018, Oliveira-Junior *et al* . 2015, Yang *et al* .

2018) and accelerating tree mortality events (Phillips *et al* . 2010, Brienen*et al* . 2015). Previous research suggests that the regulation and mobilization of non-structural carbohydrates (NSC) across plant organs is key to preventing the collapse of the plant's water transport system when faced with increasing drought stress (McDowell *et al* . 2011). However, the mechanisms of tropical forest drought-resilience are still under debate (McDowell, Brodribb & Nardini 2019, Hirota & Oliveira 2020; Janssen *et al* . 2020; Oliveira *et al* . 2021), and a comprehensive understanding of the coordination between tree carbon (C) allocation patterns in different tree organs with tree hydraulic strategies is essential to understand the response of seasonal Amazon forests to prolonged drought (Saleska *et al* . 2003; Longo *et al* . 2018, Barros *et al* . 2019).

The NSC pool maintenance can lead to higher survival rates during episodes of environmental stress (Chapin, Schulze & Mooney 1990; Niinemets, 2010). The final balance of NSC concentration in each organ is determined by the process that regulate the C-source (i.e., photosynthesis) and the components of C-sink, where in the latter case growth, respiration, secondary metabolites, and osmoregulation compete with carbon storage for future use (Chapin, Schulze & Mooney 1990; Hoch, Richter & Körner 2003; Würth, Peláez-Riedl, Wright & Körner 2005; Sala *et al.* 2010; Körner 2015). The total NSC can be partitioned into two major components: i) soluble sugar (SS), which has an immediate use in the processes of primary and secondary metabolism, or controlling the cell osmotic potential as an osmoregulator substance; and ii) starch (ST), which is an insoluble molecule mainly used as long-term C-storage reserve (Martínez-Vilalta *et al* . 2016), as transient molecules in leaves (Pelleschi *et al* . 1997; Thalmann and Santelia, 2017), and also may act as an integrator of plant metabolism and growth (Sulpice *et al* . 2009).

The concentration of the total NSC, and its components, SS and ST, is different among plant organs (i.e. leaf, branch, trunk or roots) across a variety of biomes (Würth *et al* . 2004; Martínez-Vilalta *et al* . 2016; Furze *et al* . 2018). As a less accessible C-pool, the stored NSC can remain for decades in stemwood and roots, but still represents a large portion of the total C budget (Richardson *et al* . 2013; Carbone *et al* . 2013). On the other hand, in organs such as leaves and branches, the dynamics of NSC can be highly transient with NSC storage displaying daily, seasonal or year-to-year variation in concentrations on a global scale (Martínez-Vilalta *et al* . 2016). However, a homeostatic NSC variance (synonymous to low-variability over time) has been described for leaves and branches of trees in a tropical forest in Panama during an extreme drought event induced by ENSO (Dickman *et al* . 2018). Also, in a throughfall exclusion experiment in Eastern Amazonia, the NSC reserves of trees subjected to long-term drought did not differ from those in unstressed trees (Rowland*et al* . 2015). Despite that, empirical studies of NSC dynamics at the whole-tree scale in tropical forests are rare and limited to a small number of sites, species, and tree organs (*see* Würth *et al* . 2004; O'Brien *et al* . 2015; Rowland *et al* . 2015; Dickman *et al* . 2018; Rowland *et al* . 2021; Signori-Müller*et al* . *in press*). Therefore, to gain a better understanding of NSC within each organ, it is necessary to identify environmental controls and species-specific differences determining physiological constraints on NSC storage in tropical forests, as well as the different roles played by each fraction of NSC in plant metabolism (Hartmann & Trumbore 2016).

Monitoring NSC dynamics in tree species representing a wide range of hydraulic strategies is an opportunity to understand how tropical trees respond to water stress. First, it is particularly important to link the NSC allocation pattern with plant hydraulic traits and the hydrometeorological conditions that define physiological drought experienced by the plant (McDowell *et al* . 2011, Sevanto *et al* . 2014; Anderegg *et al* . 2016; Kannenberg *et al* . 2020). Jointly, this framework may contribute to a mechanistic understanding of drought-induced tree mortality and trait selection for different aridity regimes in tropical forests (McDowell *et al* . 2018; Barros*et al* . 2019). Specifically, physiological drought is a response to plant water-use regulation that depends on the declining soil water and that determines thresholds associated with hydraulic or carbohydrate-mediated mortality (Mitchell *et al* . 2013). The link between drought-resistance strategies and C-source-sink balance is regulated by mechanisms that minimize water loss or avoid drought stress, and strategies that maximize the C-uptake to ensure reproductive success (Niinemets, 2010; Tomasella *et al* . 2020). For instance, if during a drought event water stress is too high, stomatal regulation and excessive xylem embolism disrupting transpiration flux could limit photosynthetic rates with a reduction in C-source activity; this, in turn, will lead to a negative C-balance over time that will be reflected in NSC stores (Sperry, Hack, Oren & Comstock 2002; McDowell *et al* . 2008, Sala, Piper & Hoch 2010; ; Oliveira *et al* . 2014; Rowland *et*

al . 2015). In fact, the hydraulic architecture of plants appears to be well coordinated with photosynthetic capacity at the whole plant scale in tropical forest (Santiago *et al.* 2004). In addition, a hydraulically mediated process to maintain cell turgor plays an important role in regulating tree growth that often declines in response to drought before reductions in leaf photosynthesis (Körner, 2015). Different rooting depths also contribute to the differences in the drought-resistance within tropical regions (Ivanov *et al* . 2012, Brum *et al* . 2017; Brum et al. 2019a) and might affect the NSC allocation pattern in different tree organs. Root depth ultimately interacts with the seasonal progression of soil water status, gas exchange, and NSC concentration and therefore emerges as a key trait determining tree resistance to extreme drought, and might be one of the most important traits preserving some tree species from drought-induced mortality (Nardini *et al* . 2016).

Here we aimed to understand if and how plant hydraulic strategies inferred from a suite of hydraulic traits can explain the interspecific seasonal and interannual NSC variation of trees. For the first time, we investigated the NSC concentration in different organs across a diverse number of dominant tree species (experiencing a long dry season) of an Amazonian forest in Brazil and evaluated its climate-induced variations. Specifically, we investigated how extreme drought events affect more typical seasonal dynamics of NSC and water regulation in tropical trees by sampling seasonal and interannual NSC dynamics over a three-year period, including one extreme drought period induced by the 2015 El Niño–Southern Oscillation (ENSO). The precipitation anomaly caused by the 2015 ENSO resulted in severe water stress across the eastern Amazon basin, including our study site (Jiménez-Muñoz *et al* . 2016, Brum*et al* . 2018). Specifically, we addressed two key questions: (**Q1**) How does the seasonal and interannual hydrometeorological variability affect the concentrations of starch, soluble sugar, and total NSC among organs of tree species from a seasonal Amazonian forest? **(Q2)** How do tree drought hydraulic resistance strategies affect the pattern of NSC concentration and variation in different organs across seasons and years? The overarching hypothesis in this study was that organs (leaf, branch, trunk, root) would have the highest contribution to explain the NSC, SS, and ST variability in trees, while NSC, SS and ST would differ in response to seasonality (dry and wet season) and due year-to-year variation including an extreme drought year induced by ENSO. Furthermore, the species-specific differences in drought hydraulic resistance strategies would influence the direction of change in NSC, SS, and ST concentrations in response to regular dry season and extreme drought conditions.

Methods

Site description

We performed this study at the Large-Scale Biosphere-Atmosphere Experiment in Amazonia (LBA-ECO) flux tower site in the Tapajós National Forest (BR-163 road, km67; 54°58'W, 2°51'S, Brazil). The area is located in the region of deep soil of the Barreiras formation, characterized as Dystrophic Yellow Latosol with a high fraction of clay, well-drained, presenting a moderate surface horizon (Oliveira-Junior & Correa 2001).

The region has a mean annual temperature and precipitation of 25°C and 2037 mm $year^{-1}$, respectively, and the climate is strongly seasonal with a dry season (DS) characterized by up to ~5 consecutive months (August through December) with strong reduction in monthly precipitation (Restrepo-Coupe *et al* . 2016). The forest is mostly evergreen and displays a closed canopy with a mean height of 40-45 m and is vertically structured with a high density of smaller understory trees (Rice *et al.* 2004; Stark*et al.* 2012; Smith *et al.* 2019). There is an increase in cloud cover during the wet season (WS) that reduces incoming solar radiation, while increasing the fraction of diffuse radiation (Brando*et al* . 2010). The forest phenology is driven by seasonality, typically showing a subtle but significant increase in leaf area index (LAI) from the beginning to the end of the dry season (Wu *et al* . 2016; Smith *et al* . 2019). Peak leaf-flush occurs in September, and the seasonality of leaf productivity has a negative correlation with trunk wood growth (Brando *et al* . 2010, Restrepo-Coupe *et al* . 2013, Restrepo-Coupe *et al* . 2016).

Characterization of interannual and seasonal drought stress level

A third of the Amazon rainforest is typically affected by moderate (Palmer Drought SeverityIndex - scPDSI < -2) to severe drought (scPDSI < -3), and the Tapajós forest area corresponds to the range of moderate to severe drought index (Jiménez-Muñoz *et al* . 2016). The weather is seasonal, and the wet season occurs from

January to July, while the dry season starts from August to December. Therefore, August and December represent transition periods. During our sampling effort, the water stress levels ranged from a very humid year in 2013 (CWD_{max}= 123 mm), through an intermediate intensity of water stress in 2014 (CWD_{max}= 289 mm), to an extreme drought in 2015 caused by the ENSO event (CWD_{max}= 400 mm) (Figure 1). During the 2015-2016 ENSO, the eastern Amazon exhibited extreme drought severity (scPDSI< -3) (Jiménez-Muñoz *et al* . 2016). Barros *et al* . (2019) noticed for the Tapajós forest a large variation in water availability measured by CWD during 2015-2016 ENSO. The drought had a record-breaking mean monthly temperature, with 1.5 and 2^{o}C higher than what was observed during previous ENSO events, October 1997 and January 1983, respectively (Jiménez-Muñoz *et al* . 2016).

Species selection

We selected six dominant tree species (˜35% of total forest basal area) from a long-term tree inventory database (stems [?]10 cm dbh) of permanent transects located at LBA research station, Tapajos National Forest (Pyle *et al* . 2008 updated by Longo, 2013, see Table 1). We also selected two abundant small-sized understory species (mostly with stems < 10 cm dbh), which were not included in the original forest database (Table 1). We categorized each species according to its adult tree height (H_{max}, calculated as the 95th percentile of the height values in the population) as overstory (H_{max} > 35m; trees with top canopy leaves exposed to high-light environments); midstory (H_{max}> 15-35m; trees with canopies occurring at the intermediary position along the vertical forest profile); and understory (H_{max} < 10m; trees with shaded canopy leaves rarely or never reaching the midstory) (Table 1) (Smith *et al* . 2019).

For three consecutive years (2013, 2014, and 2015) we sampled individual trees at the end of the wet season (WS; August) and dry season (DS; last week of November and the first week of December). We marked and re-visited the same individual trees across the years to sample for NSC concentration (repeated measurement, see NSC analysis below). Most of the individuals were selected and measured in our first sampling campaign (2013), however, some individuals were added in subsequent campaigns when we were able to reach the canopy of the overstory trees. We sampled 3-5 individuals of each species; a complete sampling size per species can be accessed in the supplementary SM-Table 1. None of the sampled individuals suffered noticeably damage from sampling, nor did they die during the three year sampling period

Hydraulic traits and drought-resistance strategies

We used the tree hydraulic traits together to form a single axis of drought resistance strategies (Figure 2a). All data and specific methodological explanations on how these hydraulic traits were measured can be accessed in Brum *et al* . (2019b). Importantly, we performed the NSC measurement for the same tree individuals and species during the same fieldwork as described in Brum *et al* . (2019a), only adding additional trees paired to the tagged ones to increase the sampling effort (SM-Table 1). Here, we used the species-specific vulnerability to xylem embolism assessed as the relationship between the percentage loss of xylem conductivity (PLC) and xylem water potential (Ψ). The vulnerability curve can be used to estimate the water potentials at which the tissue loses 50% (P50) and 88% (P88) of its hydraulic conductivity (Sperry *et al.* 2002). (Sperry, Hacke, Oren & Comstock 2002); higher P50 and P88 indicates greater vulnerability to xylem embolism. We also used the leaf water potential measured in the field at the peak of the dry season during a non- ENSO year (December 2014) and during the ENSO drought year (December 2015) to calculate interannual differences in the midday (12 AM - 2 PM) minimal leaf water potential (ΔLWP) measured in the field. The increase in ΔLWP represents a proxy of the interannual isohydric to anisohydric status of trees (Tardieu & Simonneau 1998), as the year-to-year minimal leaf water potential declines due to drought induced by ENSO. In addition, we used the natural-abundance of oxygen stable isotopes ($\delta^{18}O$) from xylem and soil water as a proxy to determining the depths from which plants acquire water in the soil (Dawson *et al* . 2002). According to Brum *et al* . (2019a), a fractioned evaporative gradient due an extreme drought induced by ENSO allowed us to determine a negative vector to describe the $\delta^{18}O$ (indicates that roots uptake enriched water from shallow soil, whereas deeper-rooted trees tend to present less enriched water and more negative value $\delta^{18}O$ as also observed in deeper soil.

We used this combination of functional hydraulic traits to create an index of drought-resistance and define *a posteriori* functional groups (Figure 2b). Using the matrix of species average functional hydraulic traits, we performed a principal components analysis (PCA) to create an index of drought-resistance and define a posteriori functional groups. Before running the PCA, we standardized the variables to have zero mean and unit variance. We used the scores of the first axis (PCA1), which represents the continuum of drought resistance from more negative PCA1 that summarizes the tolerance to more negative water potential, shallow root depth, and higher tolerance to xylem embolism, and to positive PCA1 describing taller drought-avoidance trees, with deeper water access and inter-annual isohydric (Figure S1). Because we did not have information on ΔLWP for *M. elata* , to perform the PCA, we replaced gaps with the average values across all species. In order to detect general groups based on hydraulic traits, we submitted the traits matrix to a hierarchical cluster analysis based on Euclidean distances, which measures pairwise dissimilarity of traits in the set for all studied species. We derived three *a posteriori* groups of species in accordance with species average functional hydraulic traits related to drought-resistance strategies (Table 1, Figure 2b). A tolerant group with *R. pubiflora* , *Miconia sp.* , *C. paniculata* with a more negatives values in PCA1 axis (Figure 2), an intermediate group with *P. apiculatum* , *C. scleroxylon* ,*A. longifolia* with positive value in PCA1 axis close to zero, and an avoidant group with *M. elata* and *E. uncinatum* higher values in PCA1. Table 1 shows that a priori canopy position height categorization, given by canopy position, not necessarily represents the drought resistance strategies in this site, mainly due the emergence of the intermediate group. We performed the PCA and cluster analysis using a basic package from R software (R Core Team 2018).

NSC analysis

For each tree, we collected samples of (a) coarse roots, by excavating close to the junction between the roots and the main trunk, up to a maximum of 30 cm depth; (b) trunk-wood tissue from 1.30 m height (up to 5 cm depth) using a 5 mm increment borer; (c) first-order branches close to the leaves, trying to sample the highest branch possible, or the most sunlight-exposed branch and leaves. We obtained branch samples using tree climbing, ladders, or pole pruners depending on the height and accessibility of the sampled trees (Table 1). In general, most of our samples were obtained at the bottom and at intermediary layers within the canopy of each individual tree. Based on previous studies showing that samples taken from full sun exposure compared to shade within the canopy had no significant effect on NSC concentrations in tropical forest trees (Würth *et al* . 2005 in Panama; and Martin *et al* . 2020 across a tropical forest elevation gradient in southern Peru). We assumed that leaves and branches from the bottom and intermediate layers would approximate the full canopy NSC storage. In addition, none of the individuals suffered noticeable damage from sampling or died during the three-year period. For more sample information and sample size see the SM-Table 1 in the supplementary material.

All samples were kept cool during the fieldwork in a cooler with ice and, on the same day, as soon as we arrived at the basecamp (lab field ˜20 km from research site), we microwaved the samples for 90 seconds at 400 W to denature enzymes that would otherwise affect NSC levels. We then dried the leaves at 65 ºC for 36 hours, starting in the evening of the sampling day (Höch *et al* . 2003).

We performed the NSC extraction in the laboratory of plant functional ecology at the University of Campinas (Campinas, SP, Brazil). We used the enzymatic method to quantify the concentrations of NSC fractions of soluble sugar and starch (see Quentin *et al* . 2015 for further discussion about NSC quantification see Höch *et al* . 2003, Dickman, Mcdowell, Sevanto, Pangle & Pockman 2015), using the following protocol: (a) we grounded leaves, wood, and root samples with their bark removed into a fine powder using the 2010 Geno/Grinder® SPEX SamplePrep. Ground samples were stored at -20 ºC until further processing. (b) We weighed approximately 14-15 mg of powdered plant material in 2 ml vials and added 1.6 mL of distilled water to each vial. (c) We incubated the vials in a water bath at 90-100 ºC for 60 minutes to solubilize sugars. Then an aliquot (700 uL) from each sample was incubated overnight to react with Amyloglucosidase from *Aspergillus niger*(Sigma-Aldrich, St. Louis, MO, USA) to breakdown the total NSC to glucose. We used the remaining aliquot volumes to determine the soluble sugar concentration using invertase from *Saccharomyces cerevisiae*(Sigma-Aldrich, St. Louis, MO, USA) to break down sucrose to fructose and glucose. Additionally,

for both reaction routines, we used GAHK (Glucose Assay Hexokinase Kit - Sigma-Aldrich, St. Louis, MO, USA) together with phosphoglucose isomerase from *Saccharomyces cerevisiae* (Sigma-Aldrich, St. Louis, MO, USA). (d) We measured the concentration of free glucose photometrically in a 96-well microplate spectrophotometer at 340 nm (EPOCH - Biotek Instruments INC - Winooski, VT - USA). (e) Finally, we calculated the starch concentration as total NSC minus soluble sugars concentration. All NSC values are expressed as the percentage of dry weight. In our analysis, we distinguished between NSC fractions by separately analyzing soluble sugar and non-soluble starch, due to their distinct role in tree physiological metabolism (Hartmann & Trumbore 2016).

Statistical analysis

In all analyses, we fitted a model for soluble sugar, starch, and NSC separately because we were interested in understanding the role of each soluble sugar separately. In addition, we calculated the fraction of average soluble sugar and starch concentration to average total NSC concentration (SS%NSC, ST%NSC). In order to answer questions 1 and 2 and identify how the different NSC, SS, and ST concentrations vary as a function of fixed effect, we performed a linear model using generalized least square (GLS) model using the function *gls* from *nlme*package (Pinheiro, Bates, DebRoy & Sakar, 2018). In this model, the errors are allowed to be correlated, present unequal variance and sample size in fixed terms. In addition, the model processes longitudinal data with repeated measurement across time, by considering a within-group correlation structure. Here, we used the compound symmetry correlation structure that corresponds to uniform correlation (*corCompSymm*function - Pinheiro, Bates, DebRoy & Sakar, 2018). For that, we considered the year of measurement as the time that co-covariate, and individuals nested within the year as the repeated measurement. We used the GLS because the starch and NSC concentration data presented a skewed distribution and in any model we tested the variance was not homogeneous. In all models evaluated we used the response variable in log scale because that reduced the AIC of the final model in contrast to the model fitted to non- log-transformed data. Therefore, in all output tables, coefficients and errors are described in log scale.

In order to answer Q1 , we first fit the GLS model using organ (leaf, branch, trunk, root) as the main fixed effect to identify the degree of difference in NSC, ST and SS allocation in each organ. After that, in order to identify the degree of difference in sugar allocation in each organ between the seasons and across the years, we fitted a model considering the interaction of season (wet, dry) and year (2013, 2014, 2015) as the fixed effect. In Q2 , we first performed a Peason correlation test between the average NSC, ST, SS, SS%NSC and ST%NSC as a function of each hydraulic trait and PCA1 axis. Our goal was to understand the overall NSCs response to the specific hydraulic traits and drought-resistance index, independently of the period sampled. Second, in order to understand the seasonal and year-to-year variability in NSC, ST, and SS concentration variance, we fitted another GLS model using drought-resistance strategy groups as the main effect (avoidant, intermediate, tolerant; Figure S1), and season and year as a fixed effect (Figure 1). We used the drought-resistance strategy groups as fixed effect in order to simplify the interaction with seasonality within each year, and variability across the years.

In order to identify the effect size and the power of results for each GLS model fitted we compare the model with the *Anova* function from the *car* package (Fox & Weisberg 2011). The function returns an analysis of deviance table (type-II test) that reports the likelihood-ratio Chi Square (hereafter denoted as X^2) and gives the effect size of the fitted model and p-value (for $p<0.05$ we accepted as statistically significant). In addition to that, for every fitted model, we performed a PostHoc test using the *emmeans*package (Lenth 2019) that estimates the marginal means (least-squared means) for specific factors or factor combinations. We used a pairwise comparison to determine specific mean differences where the p-value is adjusted in accordance with the Tukey method (hereafter denoted as $\text{PostHoc}_{\text{test}}$).

Results

Seasonal and interannual variability of non-structural carbohydrates

The mean soluble sugar to starch ratio independent of season and year was 6.4:1 in leaves, 0.9:1 in branches, 1.1:1 in trunks, and 0.5:1 in roots (Table S1). The computed estimated marginal mean of total NSC ranged

25.2 to 37.5 mg g^{-1} of dry matter for all organs sampled. There was a significant difference in SS (GLS model;X^2 =164.10, Df=3, p<0.001), ST (GLS model;X^2 =144.34, Df=3, p<0.001), and NSC (GLS model;X^2 =61.50, Df=3, p<0.001) concentrations when we evaluated organ as the unique fixed effect (Figure 3a). All organs differed in the average of SS and NSC concentrations (Table S1; Figure 3a; $PostHoc_{test}$; p <0.001). But, the concentration of ST_{leaf} was on average 5.27 mg g^{-1} lower than all other organs ($PostHoc_{test}$; p<0.001). Here, we did not observe significant pairwise differences in starch concentration among branches, trunks, and roots (PostHoc test; p<0.001). The NSC_{leaf} differed from all other organs and were an average 4.79 mg g^{-1} lower than branch and root, and 4.60 mg g^{-1} higher than trunk (PostHoc test; p<0.001). Branch and root showed similar NSC concentrations (PostHoc test; p>0.05), whereas the NSC_{trunk} concentration was on average 12.3 mg g^{-1} lower than leaves, branches, and roots (PostHoc test; p>0.05).

There was a seasonal effect modulating the concentration of SS in leaves (GLS model; X^2 =5.7, Df=1, p<0.05) and branches (GLS model; X^2 =25.7, Df=1, p<0.05) but not in trunks and roots (SM-Table 2). The interannual variability affected significantly the concentration of SS only in trunks (GLS model; X^2 =27.7, Df=2, p<0.05) and branches (GLS model; X^2 =8.1, Df=2, p<0.05), while the interaction of seasonality and interannual variability affected the concentration of SS from all organs. Despite that, the SS from all organs presented a significant variation including the interaction with seasonality and interannual variability (GLS model; Df=1, p<0.05). The SS_{leaf} was similar during the dry season and wet season of 2013 and 2014, but during ENSO year the estimated marginal mean of SS_{leaf} was 12.5 mg g^{-1} higher during dry season in contrast to wet season (PostHoc test= 12.50; SE=3.41, df=693; T ratio=-3.66; p =0.003; Figure 3b). Similarly, the main seasonal difference in $SS_{branch}$was observed during the dry season of the ENSO year (PostHoc test= -13.08; SE=2.70, df=693; T ratio=-4.48; p =0.003). Considering the inter-annual variability and comparing seasons in different years, the concentration of SS_{leaf} and SS_{branch}during the rainy season was similar during the three studied years (PostHoc test; p>0.05). However, the SS concentration during the dry season was on average 9.15 and 9 mg g^{-1}higher in leaf and branch during the ENSO year in contrast to dry season of 2013 and 2014 together (PostHoc test; p<0.001).

Trunks and roots presented the strongest interaction between season and year to explain the SS variability (SM-Table 2). There was an overall tendency in wet to dry decreases in SS_{root} and SS_{trunk} during 2013 and 2014 (PostHoc test; p<0.001), however, this pattern inverted during ENSO year (Figure 3b). The SS_{trunk} and SS_{root} were 8.84 and 10.09 mg g^{-1} higher in the dry season in contrast to the wet season in 2015, respectively (PostHoc test; p<0.001). The trunks and root present, respectively, on average 10.3 and 9.3 mg g^{-1} lower in the wet season of 2015 in contrast to the wet season from 2013 and 2014. The SS_{root} also increased in the dry season of ENSO year, there were on average 7.32 mg g^{-1} higher than the dry season of the previous year (Figure 3b).

Only the trunks presented a seasonal difference in starch concentration (GLS model; X^2 =5.7, Df=1, p<0.05), although this effect was not too strong (low X^2). In addition, both leaves (GLS model;X^2 =29.7, Df=1, p<0.05) and branches (GLS model;X^2 =12.9, Df=1, p<0.05) showed differences in starch concentration across the years. There was no significant interaction between seasons and years in all organs (Figure 3b; GLS model; p>0.05; SM-Table 2). Considering the inter-annual variability and comparing seasons among years, the ST concentration was always similar in different years (PostHoc test; p>0.05).

The variance of total NSC concentration was not explained by seasonality in all organs (SM2-Table 2). Whereas trunks (GLS model; X^2 =8.7, Df=2, p<0.05) and roots (GLS model; X^2 =11.4, Df=2, p<0.05) exhibited interannual differences in NSC concentration, only leaves (GLS model; X^2 =23.4, Df=2, p<0.05) and trunks (GLS model; X^2 =16.5, Df=2, p<0.05) presented an interaction effect between seasons and years (SM2-Table 2). During the ENSO year, the NSC_{leaf}concentration increased 11.4 mg g^{-1} during dry season in relation to wet season (PostHoc test= -11.4; SE=4.27, df=693; T ratio=-2.67; p<0.01), whereas there was no seasonal difference in NSC_{leaf} concentrations during 2013 and 2014 (PostHoc test; p>0.05). All the other organs showed no seasonal differences in NSC concentration during 2013, 2014, and 2015. In addition, considering the inter-annual variability and comparing seasons among years, the NSC concentration was always similar in different years (PostHoc test; p>0.05).

Drought-resistance strategies and non-structural carbohydrates variation

The PCA1 explained 58% the proportion of variance of the species functional hydraulic traits (Figure 2a). The drought-tolerant group is formed by shallow-rooted species, high embolism-resistance plants that also showed sharp declines (towards more negative values) in the annual minimum leaf water potential during ENSO (Figure 2b). The intermediate group included either shallow-rooted and vulnerable to xylem embolism or deep-rooted with higher resistance to xylem embolism. The drought-avoidant group was formed by overstory trees with very deep roots and high vulnerability to xylem embolism used as fixed effect (Figure 2b; S1).

The continuous PCA1 axis summarizing the drought-resistance axis was 81% and 82% negatively correlated with the average ST_{root} and total NSC_{root}, respectively (Figure 4a). Additionally, the PCA1 explained 81% and 73% of variation in the mean fraction of SS and ST with respect to total NSC in roots (Pearson correlation; $p<0.05$; SM-Table 3; Figure 4b). Among all hydraulic traits, only the ΔLWP alone presented a significant and strong relationship with SS%NSC and ST%NSC in branches and roots (SM-Table 4). Here, it is important to stress out that the sample size of this relationship was lower (n=7) than any other hydraulic traits (n=8) because we do not have ΔLWP for *Manilkara elata* . The tree maximum DBH was also negatively correlated with ST concentration in roots (SM-Table 3). In addition, we showed a significant effect of drought resistance strategy groups to explain the variation of starch and total NSC concentrations in branch, trunk and root (GLS model; $p>0.05$; SM-Table 4), but only in branch we observed a more variable concentration of ST and NSC considering the interaction between drought resistance strategy, seasonally and the year studied (GLS model; $p<0.05$).

The variance of soluble sugar in leaves, branches, trunks or roots did not differ among the drought-resistance strategy groups (GLS model; $p>0.05$; SM-Table 4; Figure 5). Only SS_{branch} presented significant change across the year (GLS model; $X^2=11.86$, Df=4, $p<0.05$; SM-Table 4), and the SS_{trunk} showed a high variability determined by the interaction between drought-resistance strategy, seasonality, and years (GLS model; $X^2=15.17$, Df=4, $p<0.05$). In particular, we did not observe seasonal differences in SS_{leaf} in the avoidant group in all studied years (PostHoc test; $p>0.05$), however, the SS_{leaf} concentration increased 10.3 mg g^{-1} in intermediate and 15.63 mg g^{-1}in the tolerant groups from wet to dry season of the ENSO year (PostHoc test; $p<0.01$). Also, both intermediate and tolerant groups presented, respectively, 8.2 and 18 mg g^{-1} of increase in SS_{branch} from wet to dry season during the ENSO year (PostHoc test; $p<0.01$). For trunks, the avoidant and intermediate trees showed higher seasonal variability in soluble sugar concentration during the dry season among all years (PostHoc; $p<0.01$). However, all groups increased on average 8.45 mg g^{-1} of the SS_{trunk} from the dry to wet season of the ENSO year (PostHoc; $p<0.01$). Trees from the intermediate group increased the SS_{root} by 13.57 mg g^{-1} from wet to dry season during the ENSO year (PostHoc; T-ratio=-4.28,$p<0.01$). In particular, during 2013 and 2014, there was an average of 7.8 mg g^{-1} decline from wet to dry season in SS_{root} (PostHoc; $p<0.05$). However, in 2015 this pattern reversed and SS_{root} increased 10.69 mg g^{-1} during the dry season in contrast to wet season (PostHoc; T-ratio=-3.24,$p<0.001$).

The ST_{leaf} and NSC_{leaf} concentrations did not differ among drought-resistance strategies, and with interactions among seasonality, drought-resistance strategy and year (GLS model; $p>0.38$; SM-Table 4). There was no particular seasonal difference in ST_{leaf} among the years ($PostHoc_{test;}$ $p>0.05$). But, during the dry season of 2015 (ENSO year), the NSC_{leaf} concentration increased in intermediate (9.6 mg g^{-1}) and in tolerant (17.9 mg g^{-1}) drought-resistance groups in contrast to the wet season of the same year (PostHoc test; $p<0.01$). The ST_{branch} was on average 13.5 mg g^{-1}higher in the drought tolerant than the average of avoidant and intermediated ST_{branch} concentration (PostHoc test; $p<0.01$). The tolerant group presented higher NSC concentration in branches than the intermediate group (PostHoc; $p<0.001$). In addition, the avoidant group contains 2.7 times higher NSC_{branch} concentrations during dry as compared to wet season, independently of the year (PostHoc; T ration=-2.97; <0.01). The avoidant group exhibited about 24.8 mg g^{-1} higher NSC_{branch} during the dry season in contrast to the wet season when we included all years together (PostHoc; $p<0.001$). In trunks, the concentration of starch and NSC was very similar among drought-resistance groups, and presented a nearly homeostatic pattern across the seasons and years.

On the other hand, the variations of ST_{root} (GLS model;X^2 =62.68, df=2,$p<0.001$) and NSC_{root}(GLS

model; X^2 =62.68, df=2,p<0.001) were strongly determined by the drought-resistance groups (Figure 5). The tolerant group showed about 45.3 mg g^{-1} higher ST_{root} concentration in contrast to the avoidant group (PostHoc; T-ratio=-7.54, p<0.01) and 34.5 mg g^{-1} higher than intermediate groups (PostHoc; T-ratio=-2.82,p<0.01). In addition, the intermediate group exhibited 10.7 mg g^{-1} higher ST_{root}than the avoidant group (PostHoc; T-ratio=-3.52 p<0.01). Similarly, all groups showed differences in contrast to NSC_{root} concentration (PostHoc; p<0.01). Even though the root system presented a rather seasonal homeostatic pattern and did not show differences across the seasons and years in ST and NSC concentration (Figure 6).

4. Discussion

We demonstrate that the concentration of SS, ST and NSC varies considerably among organs in seasonal Amazon tree species (**Q1**), confirming our initial hypothesis. Our results are in line with previous studies showing that tree organs have the highest contribution to explain the NSC variance across a diversity of biomes (Würth *et al.* 2004; Martínez-Vilalta *et al* . 2016; Furze *et al* . 2018). We also showed that the dynamics of seasonal and interannual SS concentrations in these organs was strongly affected by the extreme drought event induced by ENSO in 2015 (**Q1** ; Figure 3a). Indeed, we showed a seasonal and year-to-year homeostasis in ST and SS concentrations as observed in all organs during 2013 and 2014 (with the exception to soluble sugar in roots) (**Q1;** Figure 3b). However, the SS increased in all organs during the extreme ENSO drought, which disrupted the NSC homeostasis, while the ST concentration did not (**Q1**). An important novelty in our study is the effect that the drought-resistance strategies have on the variation of NSC concentration in some organs (**Q2**). Indeed, according to our overarching hypothesis species-specific differences in drought hydraulic resistance strategies did influence the direction of change in SS concentrations in response to regular dry season and extreme drought conditions, but not ST. The increase in SS concentration was more important in woody organs of intermediate and tolerant drought strategies during the extreme drought event. In addition, drought-resistant strategies exert a strong effect on starch and NSC concentration in roots (**Q2** ; Figure 4 and 5). These patterns suggest that contrasting drought survival strategies selected over evolutionary time scales explain part of the NSC variations. Therefore, we show for the first time that hydrological niche segregation, which determines the drought avoidance-tolerance axis of coexisting trees in Tapajós forest (Brum *et al* . 2019a), also has an important effect in determining the NSC allocation pattern in different organs and the variation in response to an extreme drought event.

NSC concentration at organ level across seasons and years

At the organ level, the average ST concentrations on leaves were lower as compared to branches, trunks and roots that showed similar average ST concentration. The ST presented more depletion than did SS, mainly in leaves and branches across the years (Figure 3; Figure S2). Moreover, the SS concentration presented the highest concentration in leaves, followed by branches, roots and trunk. The observed higher SS_{leaf} and low ST_{leaf} in our study might being reflecting the functional role of leaves that: **i**) present higher proportion of phloem tissue loading sugars towards branches as a carbon source organ, and **ii**) sustain a higher metabolic rate compared to other organs (Sala, Woodruff, Meinzer 2012; Sala and Mencuccini, 2014; Martínez-Vilalta *et al* . 2016; Guo *et al* . 2020). As starch is synthesized and degraded in chloroplasts within photosynthetic tissue at hourly basis (Santelia & Lunn 2017; Thalmann & Santelia, 2017, MacNeill *et al* . 2017), it is likely that unmeasured diurnal rhythms may affect our understanding of what determines the ST concentration in leaves in our survey, because leaves were sampled only once (at a roughly random time between 8 am to 3 pm) within each season. However, another study with 82 Amazonian species, in which the sample time was standardized, also shows higher SS concentrations in leaves than in branches (Signori-Müller *et al* . in press). Therefore, our understanding of what drives ST_{leaf} in the seasonal Amazon forest still needs increase the sampling frequency, include observations of phenological development and age-dependent leaf physiology (Albert *et al* , 2018), and perform a diurnal cycle in contrasting seasons (Gent 2018; Tixier *et al* ., 2018). We also speculate that species-specific leaf traits could also explain the differences observed in NSC among species in our site, such as observed in a tropical forest in Panama where the leaf mass per area from 23 species explained 31% of the variation of leaf total NSC concentration (Dickman *et al* . 2018); or the net leaf photosynthesis that might explain a large variation of the total ST_{leaf} concentrations (Guo *et al* . 2020).

Roots, followed by branches maintained the higher average NSC concentration, a difference mainly related to a higher allocation to ST concentration. It is well known that roots are also specialized as storage organs (Kozlowski, 1992; Aubrey & Teskey, 2018). This pattern was true for the tree species from seasonal Amazon as the coarse root system represents the main ST and NSC storage organ in our site (Table 2). Even though two species (canopy tree *Erisma uncinatum* and the understory *Amphirrhox longifolia*) present very little ST concentration in the root (Figure S3), the reasons for this observed difference is still unclear. In our study, we also showed that branches, in addition to roots have a similar average of ST concentration. A similar pattern was also described in species from a mixed temperate forest in North America (Furze *et al* . 2018), indicating the importance of branches to regulate the starch pool even in a contrasting ecosystem such as tropical forest. Also, branches are the woody organs that present the highest SS concentrations, which may indicate that branches sustain a higher metabolic rate compared to the other woody organs. In fact, branches represent the major buffer related to NSC fluctuation according to the tree water status (Woodruff & Meinzer, 2011; Dickman *et al* . 2015; Signori-Müller *et al* . in press), but also according to climatic temperature variation, leaf phenology, and changes in leaf photosynthesis rates of overstory trees in a tropical forest from Panama (Newell, Mulkey & Wright, 2002, Würth*et al* . 2005; Dickman *et al* . 2019). Compared to roots and branches, trunks have the lowest mean concentration of ST_{trunk} and SS_{trunk} (each ˜50% of the total NSC), but the percentage of SS and ST from total NSC is about 50% such as those observed in branches (Figure 6). Low concentration in NSC_{trunk} compared to the other organs reflects the relatively higher proportion of lignified and non-living tissues in trunks and sapwood as opposed to the other plant organs (Plavcová *et al* . 2016, Martínez-Vilalta *et al* . 2016; Morris *et al* . 2016). Although we measured NSC_{trunk} at a maximum of 5 cm depth in sapwood, tropical forest trees can store NSC up to 15 cm or deeper into the higher lignified sapwood (Würth *et al* . 2005) and we would expect a similar pattern in trees found in seasonal Amazon forest. In addition, the trunk is the largest fraction of tree biomass (Chave *et al* . 2014), therefore the low NSC, SS and ST concentration might be related to the trunk size relative to the rest of the plant and sugars could be more diluted along to the organ. In addition, if NSC decreases radially and such pattern is species-specific, the 5 cm deep sample could also skew the results contributing to the diverse dynamics observed in our study.

The strong drought event induced by the ENSO in 2015 disrupted the seasonal homeostasis of soluble sugar in all organs, but not the starch concentration. Overall ST concentration variation in leaves, branches and roots was not explained by seasonal and interannual variability in climatic conditions, although a weak effect was observed in the trunk. The year-to-year differences in ST concentration in leaf and branch are reflected in the prioritization of SS concentration in detriment of ST during 2015. In fact, the homeostatic pattern in ST concentration was not observed for SS, that was more variable among seasons and was driven mainly due the strong dry season during ENSO 2015 (Figure 3b). One mechanism that has been proposed to explain how plants avoid dehydration is via osmoregulation, which helps plants maintain lower turgor potentials and avoid cell water loss, reduce xylem vulnerability to cavitation, improving water uptake and allowing the plant to maintain functional metabolism during extreme drought (Morgan, 1983; Tardieu, 1996; Boyer, 1996; Sala & Mencuccini 2014; De Baerdemaeker *et al* . 2017). Indeed, during periods of water stress, changes in leaf hexose/sucrose ratios cause transient starch depletion and this shift contributes to increased osmoregulation in leaves (Pelleschi *et al* . 1997). Previous studies show that starch concentration in leaves usually decreases in response to water stress for a variety of species (Thalmann & Santelia, 2017; He *et al* . 2019; Du *et al* . 2020). In addition, as recently demonstrated by Signori-Müller *et al* . (*in press*) there is a prioritization of SS relative to ST in leaves in a broad range of taxa in the Amazon, which is coupled to tree hydraulic status, indicating the involvement of SS in the maintenance of the hydraulic function in adult tropical trees. In fact, in our dataset the proportion of ST from total NSC in leaves was the minimum during the dry season of 2015. Similarly, depletion in starch storage and increase in SS during the 2015 ENSO (Figure 1), suggests that branches are the woody organ with higher sensitivity to seasonal and year-to-year C-balance. In contrast to the other organs, branches contributed to the highest C turnover for larger scale responses over longer timescales (Trumbore 1997; Carbone *et al* . 2013; Carbone *et al* . 2016).

We described an overall tendency of the roots and trunks to decrease SS concentration from wet to dry season

in 2013 and 2014, but during the ENSO drought this pattern was inverted, and SS increased from wet to dry season in 2015. In the trunk, it is expected that endogenous and phenological rhythms might define the prioritization in carbon allocation to growth and osmoregulation might covariate with NSC cycle seasonality (Richardson *et al* ., 2013; Wagner *et al* ., 2016; Fang *et al* ., 2019). Considering that Tapajós trees exhibit low wood increment during dry season in relation to wet season at community level (Rice *et al* . 2004, Vieira *et al* . 2004), and that under water limitation the cambial activity is inhibited faster than photosynthesis during droughts (Fatichi, Leuzinger & Körner 2014, Körner, 2015), we expected that such C-sink limitation would increase ST_{trunk} as a result of the balance between reduced growth and increase storage during dry season (Sala *et al* . 2012, Wiley & Helliker, 2012, Körner, 2015; Wagner *et al* ., 2016). Also, an increase in heterotrophic trunk respiration (higher CO_2 efflux) due water deficit (Rowland *et al* ., 2018) could also down-regulate the starch storage in the trunk of Tapajós tree species. Instead, we observed a homeostatic pattern in ST concentration in the trunk, while the total NSC and soluble sugar varied with seasons and across years, but this difference was related to the prioritization of SS during the extreme drought event. To better understand all the processes that affect SS_{trunk} and ST_{trunk} dynamics, future studies should focus on the interplay between cambium phenology, wood increment rates, heterotrophic trunk respiration and changes in wood water content and NSC balance (Scartazza *et al.,* 2013, Hartmann & Trumbore 2016). In roots, we observed the lowest year-to-year seasonal changes in starch concentration, but the increase in SS in roots during the dry season might be related to water stress caused by water depletion in the clay soil matrix. Trees in our study site grow over clay soils with high water holding capacity (Oliveira-Junior & Correa, 2001, Ivanov *et al* ., 2012). If soil-root exchange is not interrupted due to increase in air gaps between roots and drying soil (Liu *et al.,* 2015), low soil water potential might induce root-to-soil water loss during the dry season (Oliveira *et al* ., 2005). An increase in SS_{roots} may be a complementary part of a mechanism exhibited by these trees to overcome the reduced soil water potential and avoid water loss to shallow dry soil during the extreme drought event of 2015. Furthermore, there is a higher interaction between soil microorganisms and root exudation production at the cost of C that may also affect the dynamics of soluble sugar (Canarini *et al* ., 2018). However, as many variables drive the strength of the C-source-sink, the feedback between climate and vegetation traits, and the NSC-balance, any attempt to explain these processes not including direct measurements of NSC falls into an unwished circularity (see Hartmann & Trumbore 2016).

Drought-resistance strategies effect in the seasonal and interannual patterns of NSC concentration

The drought-resistance strategies summarize the previous finding that distribution of leaf-area and light-environments in seasonal Amazon forests is integrally connected to **i**) tree diameter distribution (Stark *et al.,* 2015), **ii**) the effective rooting depth (Nepstad *et al* ., 1994; Markewitz *et al* ., 2010; Ivanov *et al* ., 2012), and **iii**) the coordination between rooting depth and embolism resistance suggesting a trade-off between drought avoidance (i.e. deep rooting) and drought tolerance (i.e. embolism-resistance) (Brum *et al* ., 2019a; Figure 2a). Indeed, canopy trees with greater canopy exposure to light exhibit drought-avoiding traits such as a deeper rooting which buffer the water uptake during dry season and allow a reduced investment to xylem embolism resistance and less year-to-year variation in minimal water potential during the peak of the dry season (Figure 2a). In contrast, small, shallow-rooted trees in the light-limited understory habitat exhibited the lower P50 and P88 and higher year-to-year variability in xylem water potential (Figure 2a). Here we add a novel and interesting finding to this discussion: the hydrological niche segregation (expressed by contrasting coexisting drought strategies) is also related to contrasting NSC allocation patterns. Intermediate and tolerant species exhibit higher ST storage in roots and higher remobilization to SS in all organs during water periods induced by ENSO, while the avoidant species did not show the same pattern.

Climatic regimes characterized by seasonal droughts likely select for higher NSC storage in roots of shallow-rooted trees that experience frequent reductions in soil water availability. A certain homeostasis of ST_{root} concentrations from drought-tolerant trees indicates the importance of maintaining higher starch reserves as a key component of their drought resistance strategies. Indeed, an increase in ST/NSC ratio also increases the resilience to drought-tolerant trees to less reliable water availability during dry season or less C-uptake during the rainy season due lower light availability (Huete *et al* . 2006, Restrepo-Coupe *et al* . 2016, Smith *et al* . 2019). This pattern is also associated with resprouting ability in the case of overstory branches falling

and causing stem or canopy damage to the understory species (Poorter *et al* . 2010). In addition, the stored root carbohydrates can maintain root respiration for extended periods of C-source limitation (Aubrey & Teskey, 2017) which might be an important physiological strategy for drought-tolerant species to survive in seasonal forests. These findings point to rooting depth as a key trait underlying tree resistance and resilience to extreme drought events, and is likely one of the most important traits protecting some tree species from drought-induced mortality (Nardini *et al* . 2015; Silvertown*et al.* 2015; Chitra-Tarak *et al.* 2017), or selecting for drought-persistence in Tapajós forest (Brum *et al.* 2019a). But also, the higher ST and NSC concentration in branches of drought tolerant species that support more decrease in leaf water potential (SM-Table 3) represent a new perspective to understand the covariation effect between C-allocation and drought-resistance strategies in branches also. It seems that the survival of species relying only on shallow soil water resources requires mechanisms to buffer the environmental stresses by guaranteeing higher ST storage. Indeed, shallow-rooted drought-tolerant species experience seasonal root water stress, low radiation availability inhibiting the high accumulation of photosynthates.

The temporal variation in water stress induced by ENSO determines higher remobilization to SS in all organs in species of intermediate and high drought tolerance. The seasonal changes in soluble sugar from the intermediate and tolerant plants during an extreme drought, also reveal ecological implications related to the ecohydrological niches of species and the need for species to present short-term physiological adjustments to survive during an extreme drought event. While the deeply rooted and drought-avoidant trees can buffer water stress, trees whose roots are limited to shallow soil, where the effect of drought can be stronger, needed a whole plant osmotic adjustment reflecting the SS increase in all organs. In fact, the shallow rooted drought-tolerant species that face lower water variability during the extreme drought also prioritize SS relative to ST in the whole plant, reflecting a mechanism that increases the osmoregulation of these trees (Sala *et al* . 2012; He*et al* . 2020). These results suggest that an increase in C-pool of stored reserves represent a key drought-resistance trait as it provides the necessary SS for the maintenance of whole plant cell turgor and vascular integrity under adverse environmental conditions (Morgan, 1984; Turner, 2018, Sala *et al* . 2012; Dickman *et al* . 2015; Guo*et al* . 2019). These results also suggest that species that are more adapted to seasonal and year-to-year variation in water deficit may have higher ability to rapidly adjust the whole plant SS concentration under extreme water stress.

5.1 Conclusion

The high interspecific variation in NSC fluctuations observed in this study likely represents the diversity of evolutionary adaptation to cope with drought within this taxonomically diverse tropical forest. Interestingly, no strong depletion of NSC was observed at any time, most likely because an increased investment in soluble sugars was a uniform response in all organs during the 2015 ENSO extreme drought. This event disrupted the regular year-to-year SS homeostasis observed in regular years. The link between soluble sugar and water stress was especially important for branches, trunks, and roots of species of intermediate and high drought tolerance. A final important finding was the consistent pattern of starch storage exhibited by drought-tolerant species. It seems that the persistence in seasonal tropical forest understories requires high tolerance of environmental stresses, obtained in part by increasing soluble sugar during water stress, and maintaining high starch concentration in roots. Indeed, shallow-rooted drought-tolerant species experience seasonal root water stress, low radiation availability inhibiting the high accumulation of photosynthates. In general, when abiotic conditions constrain growth due to high C-source limitation, NSC responses depend on hydraulic traits and physiological regulation patterns which have been selected to increase survival under reduced productivity.

Acknowledgement

We are grateful to the LBA-INPA assistance in Santarém with special respect to Louro Lima. We would also like to thank Sky Dominguez for the manager's support. The authors confirm they do not have any conflict of interest.

Funding

This study was financed in part by the Coordenação de Aperfeiçoamento de Pessoal de Nível Superior - Brasil (CAPES) - Finance Code 001 for MB, CS-M and DP PhD project, by the Go-Amazon project (FAPESP 2013/50533-5 and U.S. DOE grant # DE. SC0008383), and by U.S. National Science Foundation (NSF) award #1754183. CS-M thanks the Brazilian National Council for Scientific and Technological Development for a scholarship (CNPq 140353/2017-8) and R.S.O for a CNPq productivity scholarship. R.S.O thanks FAPESP/Microsoft research (grant 11/52072-0). VI acknowledges the support of the NSF DEB Grant 1754163 and U.S. Department of Energy OBER Grant DESC0011078.

References

Reference

Albert L.P., Wu J., Prohaska N., de Camargo P.B., Huxman T.E., Tribuzy E.S., Ivanov V.Y., Oliveira R.S., Garcia S., Smith M.N., Oliveira-Junior R.C., Restrepo-Coupe N., da Silva R., Stark S.C., Martins G.A., Penha D.V. & Saleska S.R. (2018). Age-dependent leaf physiology and consequences for crown-scale carbon uptake during the dry season in an Amazon evergreen forest. *New Phytologist* 219, 870–884. Allen C.D., Breshears D.D. & McDowell N.G. (2015). On underestimation of global vulnerability to tree mortality and forest die-off from hotter drought in the Anthropocene. *Ecosphere* 6, 1–55. Anderegg W.R.L., Klein T., Bartlett M., Sack L., Pellegrini A.F.A., Choat B. & Jansen. S. (2016). Meta-analysis reveals that hydraulic traits explain cross-species patterns of drought-induced tree mortality across the globe. *Proceedings of the National Academy of Sciences*113, 2–7. Aubrey D.P. & Teskey R.O. (2018) Stored root carbohydrates can maintain root respiration for extended periods. New Phytologist 218, 142–152. Barros F.V.., Bittencourt P.R.L., Brum M., Restrepo-Coupe N., Pereira L., Teodoro G.S., Saleska S.R., Borma L.S., Christoffersen B.O., Penha D., Alves L.F., Lima A.J.N., Carneiro V.M.C., Gentine P., Lee J., Aragao L.E.O.C., Ivanov V., Leal L.S.M., Araujo A.C. & Oliveira R.S. (2019). Hydraulic traits explain differential responses of Amazonian forests to the 2015 El Nino-induced drought. *New Phytologist* 223, 1253–1266. Boyer J.S. (1996). Advances in Drought Tolerance in Plants.*Advances in Agronomy* 56, 187-218 Brando P.M.,. Goetz S.J., Baccini A., Nepstad D.C., Beck P.S.A. & Christman M.C. (2010). Seasonal and interannual variability of climate and vegetation indices across the Amazon. *Proceedings of the National Academy of Sciences* 107, 14685–14690. Brienen R.J.W., Phillips O.L., Feldpausch T.R et al. (2015). Long-term decline of the Amazon carbon sink. *Nature* 519, 344–8. Brum M., Teodoro G.S., Abrahao A. & Oliveira R.S. (2017) Coordination of rooting depth and leaf hydraulic traits defines drought-related strategies in the campos rupestres, a tropical montane biodiversity hotspot. Plant and Soil 420, 467–480. Brum M., Gutierrez-Lopez J., Asbjornsen H., Licata J., Pypker T., Sanchez G. & Oliveira R.S. (2018). ENSO effects on the transpiration of eastern Amazon trees. *Philosophical transactions of the Royal Society of London Series B, Biological sciences* 373:20180085. Brum M., Vadeboncoeur M.A., Ivanov V., Asbjornsen H., Saleska S., Alves L.F., Penha D., Dias J.D., Aragao L.E.O.C., Barros F., Bittencourt P., Pereira L. & Oliveira R.S. (2019a). Hydrological niche segregation defines forest structure and drought tolerance strategies in a seasonal Amazon forest. *Journal of Ecology* 107(1), 1–16. Brum M. et al. (2019b). Data from: Hydrological niche segregation defines forest structure and drought tolerance strategies in a seasonal Amazon forest, Dryad, Dataset, https://doi.org/10.5061/dryad.v704dj2 Canarini A., Kaiser C., Merchant A., Richter A. & Wanek W. (2019) Root exudation of primary metabolites: Mechanisms and their roles in plant responses to environmental stimuli. Frontiers in Plant Science 10. Carbone M.S., Czimczik C.I., Keenan T.F., Murakami P.F., Pederson N., Schaberg P.G., Xu X. & Richardson A.D. (2013). Age, allocation and availability of nonstructural carbon in mature red maple trees.*New Phytologist* 200:1145–1155. Carbone M.S., Richardson A.D., Chen M., Davidson E.A., Hughes H., Savage K.E. & Hollinger D.Y. (2016). Constrained partitioning of autotrophic and heterotrophic respiration reduces model uncertainties of forest ecosystem carbon fluxes but not stocks. Journal of Geophysical Research:*Biogeosciences* 121(9), 2476-2492. Chapin F.S., Schulze E.-D. & Mooney H.A. (1990). The Ecology and Economics of Storage in Plants. *Annual Review of Ecology and Systematics* 21, 423–447. Chave J., Rejou-Mechain M., Burquez A., Chidumayo E., Colgan M.S., Delitti W.B.C., ... Vieilledent G. (2014) Improved allometric models to estimate the aboveground biomass of tropical trees. Global Change Biology 20, 3177–3190. Chitra-Tarak R., Ruiz L., Dattaraja H.S., Kumar M.S.M., Riotte J., Suresh H.S., McMahon S.M. & Sukumar R. (2017). The roots of the drought: Hydrology

and water uptake strategies mediate forest-wide demographic response to precipitation. *Journal of Ecology* 12, 3218–3221. Dawson T.E., Mambelli S., Plamboeck A.H., Templer P.H. & Tu K.P. (2002). Stable isotopes in plant ecology. *Annual review of ecology and systematics* 33, 507–559. De Baerdemaeker N.J.F., Salomon R.L., De Roo L. & Steppe K. (2017). Sugars from woody tissue photosynthesis reduce xylem vulnerability to cavitation. *New Phytologist* 216, 720–727. Dickman L.T., Mcdowell N.G., Sevanto S., Pangle R.E. & Pockman W.T. (2015) Carbohydrate dynamics and mortality in a pinon-juniper woodland under three future precipitation scenarios. *Plant, Cell and Environment* 38(4), 729-739. Dickman, L.T., McDowell, N.G., Grossiord, C., Collins, A.D., Wolfe, B.T., Detto, M., Wright S.J., Medina-Vega J.A., Goodsman D., Rogers A., Serbin S.P., Wu J., Ely K.S., Michaletz S.T., Xu C., Kueppers L. & Chambers J.Q. (2019). Homoeostatic maintenance of nonstructural carbohydrates during the 2015–2016 El Nino drought across a tropical forest precipitation gradient. Plant, cell & environment, 42(5), 1705-1714. Doughty C.E., Metcalfe D.B., Girardin C.A.J. et al. (2015). Drought impact on forest carbon dynamics and fluxes in Amazonia. *Nature*519(7541), 78-82. Du Y., Lu R. & Xia J. (2020). Impacts of global environmental change drivers on non-structural carbohydrates in terrestrial plants.*Functional Ecology* doi:10.1111/1365-2435.1357 Fang J., Lutz J.A., Shugart H.H. & Yan X. (2020) A physiological model for predicting dynamics of tree stem-wood non-structural carbohydrates. Journal of Ecology 108, 702–718. Fatichi S., Leuzinger S. & Korner C. (2014) Moving beyond photosynthesis: From carbon source to sink-driven vegetation modeling.*New Phytologist* 201, 1086–1095. Fox J. & Weisberg S. (2011). An R Companion to Applied Regression, Second Edition. Thousand Oaks CA: Sage. URL: http://socserv.socsci.mcmaster.ca/jfox/Books/Companion Furze M.E., Huggett B.A., Aubrecht D.M., Stolz C.D., Carbone M.S. & Richardson A.D. (2018) Whole-tree nonstructural carbohydrate storage and seasonal dynamics in five temperate species. *New Phytologist* 221, 1466-1477. Gent M.P.N. (2018) Dynamic carbohydrate supply and demand model of vegetative growth: response to temperature, light, carbon dioxide, and day length. Agronomy 8. Guo J.S., Gear L., Hultine K.R., Koch G.W. & Ogle K. (2020) Non-structural carbohydrate dynamics associated with antecedent stem water potential and air temperature in a dominant desert shrub. Plant Cell and Environment 43, 1467–1483. Hartmann H. & Trumbore S. (2016) Understanding the roles of nonstructural carbohydrates in forest trees – from what we can measure to what we want to know. *New Phytologist* 211, 386–403. Hartmann H., Moura C.F., Anderegg W.R.L., Ruehr N.K., Salmon Y., Allen C.D., Arndt S.K., Breshears D.D., Davi H, Galbraith D., Ruthrof K.X., Wunder J., Adams H.D., Bloemen J., Cailleret M., Cobb R., Gessler A., Grams T.E.E., Jansen S., Kautz M., Lloret F. & O'Brien M. (2018). Research frontiers for improving our understanding of drought-induced tree and forest mortality. *New Phytologist* 218, 15–28. He W., Liu H., Qi Y., Liu F. & Zhu X. (2020) Patterns in nonstructural carbohydrate contents at the tree organ level in response to drought duration. Global Change Biology 26, 3627–3638. Hirota M. & Oliveira R, (2020) Crossing thresholds on the way to ecosystem shifts. *Science*, 367(6479), 739-740. Hoch G., Richter A., Korner C. (2003). Non-structural carbon compounds in temperate forest trees. *Plant, Cell and Environment*26(7):1067-1081. Huete A.R., Didan K., Shimabukuro Y.E., Ratana P., Saleska S.R., Hutyra L.R., . . . Myneni R. (2006) Amazon rainforests green-up with sunlight in dry season. *Geophysical Research Letters* **33**, 2–5. Ivanov V.Y., Hutyra L.R., Wofsy S.C., Munger J.W., Saleska S.R., De Oliveira R.C. & De Camargo P.B. (2012). Root niche separation can explain avoidance of seasonal drought stress and vulnerability of overstory trees to extended drought in a mature Amazonian forest.*Water Resources Research* 48(12). Janssen T., Fleischer K., Luyssaert S., Naudts K. & Dolman H. (2020) Drought resistance increases from the individual to the ecosystem level in highly diverse neotropical rain forest: a meta-analysis of leaf, tree and ecosystem responses to drought. Biogeosciences Discussions 17:2621–26451-41. https://doi.org/10.5194/bg-17-2621-2020 Jimenez-Munoz J.C., Mattar C., Barichivich J., Santamaria-Artigas A., Takahashi K., Malhi Y., Sobrino J.A. & Schrier G Van Der (2016). Record-breaking warming and extreme drought in the Amazon rainforest during the course of El Nino 2015-2016. *Scientific Reports* 6, 333130. Kannenberg S.A. & Phillips R.P. (2020). Non-structural carbohydrate pools not linked to hydraulic strategies or carbon supply in tree saplings during severe drought and subsequent recovery. *Tree Physiol* 40, 259–271. Korner C. (2015). Paradigm shift in plant growth control. *Current Opinion in Plant Biology* 25, 107–114. Kozlowski T.T. (1992). Carbohydrate sources and sinks in woody plants.*The Botanical Review* 58(2), 107-222. Lenth R. (2019). emmeans: Estimated Marginal Means, aka Least-Squares Means. R package version 1.4.1. https://CRAN.R-project.org/package=emmeans Liu

X.P., Zhang W.J., Wang X.Y., Cai Y.J. & Chang J.G. (2015). Root-soil air gap and resistance to water flow at the soil-root interface of Robinia pseudoacacia. *Tree Physiology* 35(12), 1343-1355. Longo M. (2013). Amazon forest response to changes in rainfall re- gime: Results from an individual-based dynamic vegetation model.*Dissertation Thesis, Harvard University*. Longo M., Knox R.G., Levine N.M., Alves L.F., Bonal D., Camargo P.B., Fitzjarrald D.R., Hayek M.N., Restrepo-Coupe N., Saleska S.R., da Silva R., Stark S.C., Tapajos R.P., Wiedemann K.T., Zhang, K. Wofsy S.C. & Moorcroft P.R. (2018). Ecosystem heterogeneity and diversity mitigate Amazon forest resilience to frequent extreme droughts. *New Phytologist* 219, 914-931. Longo, M., Saatchi, S., Keller, M., Bowman, K., Ferraz, A., Moorcroft, P. R., et al. (2020). Impacts of degradation on water, energy, and carbon cycling of the Amazon tropical forests. *Journal of Geophysical Research: Biogeosciences* 125, e2020JG005677. MacNeill G.J., Mehrpouyan S., Minow M.A.A., Patterson J.A., Tetlow I.J. & Emes M.J. (2017). Starch as a source, starch as a sink: The bifunctional role of starch in carbon allocation. *Journal of experimental botany* 68(16), 4433-4453. Marengo J.A., Tomasella J., Alves L.M., Soares W.R. & Rodriguez D.A. (2011). The drought of 2010 in the context of historical droughts in the Amazon region. *Geophysical Research Letters* 38(12). Markewitz D., Devine S., Davidson E.A., Brando P. & Nepstad D.C. (2010) Soil moisture depletion under simulated drought in the Amazon: Impacts on deep root uptake. New Phytologist 187, 592–607. Martin R.E., Asner G.P., Bentley L.P., Shenkin A., Salinas N., Huaypar K.Q., ... Malhi Y. (2020) Covariance of Sun and Shade Leaf Traits Along a Tropical Forest Elevation Gradient. Frontiers in Plant Science 10, 1–13. Martinez-Vilalta J., Sala A., Asensio D., Galiano L., Hoch G., Palacio S., Piper F.I. & Lloret F. (2016). Dynamics of non-structural carbohydrates in terrestrial plants: a global synthesis.*Ecological Monographs* 86, 495–516. McDowell N.G., Beerling D.J., Breshears D.D., Fisher R.A. & Raffa K.F., Stitt M. (2011). The interdependence of mechanisms underlying climate-driven vegetation mortality. *Trends in Ecology & Evolution* 26, 523–532. McDowell N.G., Brodribb T.J. & Nardini A. (2019). Hydraulics in the 21 st century. *New Phytologist* 224, 537–542. Mitchell P.J., O'Grady A.P., Tissue D.T., White D.A., Ottenschlaeger M.L. & Pinkard E.A. (2013). Drought response strategies define the relative contributions of hydraulic dysfunction and carbohydrate depletion during tree mortality. *New Phytologist* 197, 862–872. . Morgan J.M. (1983). Osmoregulation as a selection criterion for drought tolerance in wheat. *Australian Journal of Agricultural Research*34(6), 607-614. Morris H., Plavcova L., Cvecko P., Fichtler E., Gillingham M.A.F., Martinez-Cabrera H.I., Mcglinn D.J., Wheeler E., Zheng J., Ziemińska K. & Jansen S. (2016). A global analysis of parenchyma tissue fractions in secondary xylem of seed plants. *New Phytologist*, 209(4), 1553-1565. Nardini A., Casolo V., Dal Borgo A., Savi T., Stenni B., Bertoncin P., ... Mcdowell N.G. (2016) Rooting depth, water relations and non-structural carbohydrate dynamics in three woody angiosperms differentially affected by an extreme summer drought. Plant, Cell and Environment 39, 618–627. Nepstad D.C., de Carvalho C.R., Davidson E.A., Jipp P.H., Lefebvre P.A., Negreiros G.H., da Silva E.D., Stone T.A. & Trumbore S.E., Vieira S. (1994). The role of deep roots in the hydrological and carbon cycles of Amazonian forests and pastures. *Nature* 372, 666–669. Newell E.A., Mulkey S.S. & Wright S.J. (2002). Seasonal patterns of carbohydrate storage in four tropical tree species. *Oecologia*131(3), 333-342. Niinemets Ü. (2010) Responses of forest trees to single and multiple environmental stresses from seedlings to mature plants: Past stress history, stress interactions, tolerance and acclimation. Forest Ecology and Management 260, 1623–1639. O'Brien M.J., Burslem D.F.R.P., Caduff A., Tay J. & Hector A. (2015). Contrasting nonstructural carbohydrate dynamics of tropical tree seedlings under water deficit and variability. *New Phytol* 205, 1083–1094. Oliveira R.S., Dawson T.E., Burgess S.S.O. & Nepstad D.C. (2005). Hydraulic redistribution in three Amazonian trees. *Oecologia* 145, 354–363. . Oliveira R.S., Christoffersen B.O., de V. Barros F., Teodoro G.S., Bittencourt P., Brum-Jr M.M. & Viani R.A.G. (2014) Changing precipitation regimes and the water and carbon economies of trees. Theoretical and Experimental Plant Physiology 26, 65–82. Oliveira, R. S., Eller, C. B., Barros, F. D. V., Hirota, M., Brum, M., & Bittencourt, P. (2021). Linking plant hydraulics and the fast-slow continuum to understand resilience to drought in tropical ecosystems. New Phytologist*https://doi.org/10.1111/nph.17266*Oliveira-Junior R.C. & Correa J.R.V. (2001). Aptidao agricola dos solos do municipio de Belterra, Estado do Para. *Embrapa Amazonia Oriental-Documentos* (INFOTECA-E). Oliveira-Junior, R.C.D.O., Keller M.M., Ramos J.F.D.F., Beldini T.P., Crill P.M., Camargo P.B.D. & Haren J.V. (2015). Chemical analysis of rainfall and throughfall in the Tapajos National Forest, Belterra, Para, Brazil. *Revista Ambiente & Agua,* 10(2), 263-285. Pelleschi S.,

Rocher J.P. & Prioul J.L. (1997). Effect of water restriction on carbohydrate metabolism and photosynthesis in mature maize leaves. *Plant, Cell & Environment, 20, 493-503.*Phillips O.L., van der Heijden G. & Lewis S.L. et al. (2010). Drought–mortality relationships for tropical forests. *New Phytologist* 187, 631–646. Pinheiro J., Bates D., DebRoy S., Sarkar D., R Core Team (2018). _nlme: Linear and Nonlinear Mixed Effects Models_. R package version 3.1-137, <URL:*https://CRAN.R-project.org/package=nlme*>. Plavcova L., Hoch G., Morris H., Ghiasi S. & Jansen S. (2016). The amount of parenchyma and living fibers affects storage of nonstructural carbohydrates in young stems and roots of temperate trees.*American journal of botany* 103, 603-612. Poorter L., Kitajima K., Mercado P., Chubina J., Melgar I. & Prins H.H.T. (2010). Resprouting as a persistence strategy of tropical forest trees: Relations with carbohydrate storage and shade tolerance.*Ecology*, 91(9), 2613-2627. Pyle E.H., Santoni G.W., Nascimento H.E.M., Hutyra L.R., Vieira S., Curran D.J., Van Haren J., Saleska S.R., Chow V.Y., Camargo P.B., Laurance W.F. & Wofsy S.C. (2008). Dynamics of carbon, biomass, and structure in two Amazonian forests. *Journal of Geophysical Research: Biogeosciences* 113, G00B08 Quentin A.G., Pinkard E.A. & Ryan M.G. et al. (2015). Non-structural carbohydrates in woody plants compared among laboratories. *Tree Physiology* 35, 1146–1165. R Core Team (2017). R: A language and environment for statistical com- puting. Vienna, Austria: R Foundation for Statistical Computing. Retrieved from https://www.R-project.org/ Restrepo-Coupe N., Levine N.M., Christoffersen B.O., Albert L.P., Wu J., Costa M.H., Galbraith D., Imbuzeiro H., Martins G., da Araujo A.C., Malhi Y.S., Zeng X., Moorcroft P & Saleska S.R. (2016). Do dynamic global vegetation models capture the seasonality of carbon fluxes in the Amazon basin? A data-model intercomparison. *Global Change Biology*23, 191–208. Restrepo-Coupe N., da Rocha H.R., Hutyra L.R., da Araujo A.C., Borma L.S., Christoffersen B., Cabral O.M.R.R., de Camargo P.B., Cardoso F.L., da Costa A.C.L., Fitzjarrald D.R., Goulden M.L., Kruijt B., Maia J.M.F.F., Malhi Y.S., Manzi A.O., Miller S.D., Nobre A.D., von Randow C., Sa L.D.A., Sakai R.K., Tota J., Wofsy S.C., Zanchi F.B. & Saleska S.R. (2013). What drives the seasonality of photosynthesis across the Amazon basin? A cross-site analysis of eddy flux tower measurements from the Brazil flux network. *Agricultural and Forest Meteorology*182–183, 128–144. Rice A.H., Pyle E.H., Saleska S.R., Hutyra L., Palace M., Keller M., De Camargo P.B., Portilho K., Marques D.F. & Wofsy S.C. (2004). Carbon balance and vegetation dynamics in an old-growth Amazonian forest.*Ecological Applications,* 14(4), 55-71. Richardson A.D., Carbone M.S., Keenan T.F., Czimczik C.I., Hollinger D.Y., Murakami P., Schaberg P.G. & Xu X. (2013). Seasonal dynamics and age of stemwood nonstructural carbohydrates in temperate forest trees.*New Phytologist* 197, 850–861. Rowland L., da Costa A.C.L., Galbraith D.R., Oliveira R.S., Binks O.J., Oliveira A.A.R., Pullen A.M., Doughty C.E., Metcalfe D.B., Vasconcelos S.S., Ferreira L.V., Malhi Y., Grace J., Mencuccini M. & Meir P. (2015). Death from drought in tropical forests is triggered by hydraulics not carbon starvation. *Nature* 528, 119–122. Rowland L., da Costa A.C.L., Oliveira A.A.R., Oliveira R.S., Bittencourt P.L., Costa P.B., Giles A.L., Sosa A.I., Coughlin I., Godlee J.L., Vasconcelos S.S., Junior J.A.S., Ferreira L.V., Mencuccini M. & Meir P. (2018). Drought stress and tree size determine stem CO2 efflux in a tropical forest. *New Phytologist* 218, 1393-1405. Rowland L., da Costa A.C.L., Oliveira R.S., Bittencourt P.R.L., Giles A.L., Coughlin I., ... Meir P. (2021). The response of carbon assimilation and storage to long-term drought in tropical trees is dependent on light availability. *Functional Ecology* 35, 43–53. Sala A. & Mencuccini M. (2014).Ecosystem science: Plump trees win under drought. *Nature Climate Change*, 4(8), 666-667. Sala A., Piper F. & Hoch G. (2010).Physiological mechanisms of drought-induced tree mortality are far from being resolved. *New Phytologis*t 186, 274–281. Sala A., Woodruff D.R. & Meinzer F.C. (2012) Carbon dynamics in trees: feast or famine? *Tree Physiology* 32:764–775. Saleska S.R., Miller S.D., Matross D.M., Goulden M.L., Wofsy S.C., Da Rocha H.R., De Camargo P.B., Crill P., Daube B.C., De Freitas H.C., Hutyra L., Keller M., Kirchhoff V., Menton M., Munger J.W., Pyle E.H., Rice A.H. & Silva H. (2003). Carbon in Amazon Forests: Unexpected Seasonal Fluxes and Disturbance-Induced Losses. *Science,*302(5650), 1554-1557. Santelia D. & Lunn J.E. (2017). Transitory Starch Metabolism in Guard Cells: Unique Features for a Unique Function. *Plant Physiology*174(2), 539-549. Santiago L.S., Goldstein G., Meinzer F.C., Fisher J.B., Machado K., Woodruff D. & Jones T. (2004) Leaf photosynthetic traits scale with hydraulic conductivity and wood density in Panamanian forest canopy trees. Oecologia 140, 543–550. Scartazza A., Moscatello S., Matteucci G., Battistelli A. & Brugnoli E. (2013). Seasonal and inter-annual dynamics of growth, non-structural carbohydrates and C stable isotopes in a Mediterranean beech

forest.*Tree physiology*, 33(7), 730-742. Sevanto S., Mcdowell N.G., Dickman L.T., Pangle R. & Pockman W.T. (2014). How do trees die? A test of the hydraulic failure and carbon starvation hypotheses. *Plant, Cell & Environment* 37, 153–161. Signori-Muller, C., Oliveira, R.S., de Vasconcellos Barros, F. et al. (40 more authors) (Accepted: 2021) Non-structural carbohydrates mediate seasonal water stress across Amazon forests. Nature Communications. ISSN 2041-1723 (In Press) Silvertown J., Araya Y. & Gowing D. (2015). Hydrological niches in terrestrial plant communities: A review. *Journal of Ecology* 103, 93–108. Smith M.N., Stark S.C., Taylor T.C., Ferreira M.L., Oliveira E., Restrepo-Coupe N., Chen S., Woodcock T., Santos D.B., Alves L.F, Figueira M., Camargo P.B., Oliveira R.C., Aragao L.E.O.C., Falk D.A., McMahon S.M., Huxman T.E. & Saleska SR (2019). Seasonal and drought-related changes in leaf area profiles depend on height and light environment in an Amazon forest. *New Phytologist* 222, 1284–1297. Sperry J.S., Hacke U.G., Oren R. & Comstock J.P. (2002). Water deficits and hydraulic limits to leaf water supply. *Plant, Cell and Environment* 25, 251–263. Stark S.C., Leitold V., Wu J.L., Hunter M.O., de Castilho C. V., Costa F.R.C., McMahon S.M., Parker G.G., Shimabukuro M.T., Lefsky M.A., Keller M., Alves L.F., Schietti J., Shimabukuro YE, Brandao DO, Woodcock TK, Higuchi N, de Camargo PB, de Oliveira R.C, & Saleska S.R. (2012). Amazon forest carbon dynamics predicted by profiles of canopy leaf area and light environment Chave J (ed). *Ecology Letters* 15, 1406–1414. Sterck F., Markesteijn L., Schieving F. & Poorter L. (2011). Functional traits determine trade-offs and niches in a tropical forest community.*Proceedings of the National Academy of Sciences* 108, 20627–20632. Sombroek W. (2001). Spatial and Temporal Patterns of Amazon Rainfall. AMBIO A. J. Hum *Environ* 30, 388–396. Sulpice R., Pyl E.T., Ishihara H., Trenkamp S., Steinfath M., Witucka-Wall H., Gibon Y., Usadel B., Poree F., Piques M.C., Von Korff M., Steinhauser M.C., Keurentjes J.J.B., Guenther M., Hoehne M., Selbig J., Fernie A.R., Altmann T. & Stitt M (2009). Starch as a major integrator in the regulation of plant growth. *Proceedings of the National Academy of Sciences* 106, 10348–10353. Tardieu F. (1996). Drought perception by plants Do cells of droughted plants experience water stress? *Plant Growth Regulation* 20, 93–104. Tardieu F. & Simonneau T. (1998) Variability among species of stomatal control under fluctuating soil water status and evaporative demand: modelling isohydric and anisohydric behaviours. Journal of Experimental Botany 49, 419–432. Tixier A., Orozco J., Roxas A.A., Earles J.M. & Zwieniecki M.A. (2018) Diurnal variation in nonstructural carbohydrate storage in trees: Remobilization and vertical mixing. Plant Physiology 178, 1602–1613. Thalmann M. & Santelia D. (2017). Starch as a determinant of plant fitness under abiotic stress. *New Phytologist* 214, 943–951. Tomasella M., Petrussa E., Petruzzellis F., Nardini A. & Casolo V. (2020). The possible role of non-structural carbohydrates in the regulation of tree hydraulics. International Journal of Molecular Sciences 21. Trumbore S.E. (1997). Potential responses of soil organic carbon to global environmental change. *Proceedings of the National Academy of Sciences* 94(16), 8284-8291. Vieira, S., de Camargo, P. B., Selhorst, D., Da Silva, R., Hutyra, L., Chambers, J.Q., Brwon I.F., Higuchi N., dos Santos, J., Wofsy S.C., Trumbore, S.E. & Martinelli L.A. (2004). Forest structure and carbon dynamics in Amazonian tropical rain forests. *Oecologia* 140, 468–479. Wagner F.H., Herault B. & Bonal D, et al. (2016). Climate seasonality limits leaf carbon assimilation and wood productivity in tropical forests. *Biogeosciences* 13, 2537–2562. Wiley E. &Helliker B. (2012). A re-evaluation of carbon storage in trees lends greater support for carbon limitation to growth. *New Phytologist*, 195(2), 285-289. Woodruff D.R. & Meinzer F.C. (2011) Water stress, shoot growth and storage of non-structural carbohydrates along a tree height gradient in a tall conifer. Plant, Cell and Environment 34, 1920–1930. Wu J., Albert L.P., Lopes A.P., Restrepo-Coupe N., Hayek M., Wiedemann K.T., Guan K., Stark S.C., Christoffersen B., Prohaska N., Tavares J. V., Marostica S., Kobayashi H., Ferreira M.L., Campos K.S., Silva R. da, Brando P.M., Dye D.G., Huxman T.E., Huete A.R., Nelson B.W, Saleska S.R., da Silva R., Brando P.M., Dye D.G., Huxman T.E., Huete A.R., Nelson B.W. & Saleska S.R. (2016). Leaf development and demography explain photosynthetic seasonality in Amazon evergreen forests.*Science* 351, 972–976. Wurth M.K.R., Pelaez-Riedl S., Wright S.J. & Korner C. (2005). Non-structural carbohydrate pools in a tropical forest. *Oecologia*143, 11–24. Yang Y., Saatchi S.S., Xu L., Yu Y., Choi S., Phillips N., Kennedy R., Keller M., Knyazikhin Y. & Myneni R.B. (2018). Post-drought decline of the Amazon carbon sink. *Nature communications* 9(1), 1-9.

List of Table

Table 1 Biological and structural attributes of the species studied at the Tapajos Forest km 67 LBA study

area, Brazil. Values for basal area abundance are averages across a 4-ha survey area of all trees larger than 10 cm in diameter at breast height. Two understory species (*A. longifolia* and *R. pubiflora*) were recorded in five 0.05-ha plots. Species are listed from the deepest rooted species at the top to the shallowest rooted species at the bottom, as determined in Brum *et al* . (2019). The maximum height attained (H_{max}, m) per species was calculated as the 95^{th} percentile of the distribution of heights generated by a model fitting a height-stem diameter relationship at the study site (Longo *et al* . 2020). For the understory species, H_{max} was calculated from direct height measurements (M. Brum, unpublished).

Species*	**Family**	**Hmax (m)**	**Canopy Position**	**Drought resistance group**	**Basal Area ($m^2.ha^{-1}$)**	**Abundance ($ind.ha^{-1}$)**
Manilkara elata (Allemão ex Miq.) Monach[1]	Sapotaceae	41.8	overstory	avoidant	2.19	10.5
Erisma uncinatum Warm.	Vochysiaceae	48.8	overstory	avoidant	3.64	11.0
Chamaecrista scleroxylon (Ducke) H.S.Irwin and Barneby[2]	Leguminosae	35.2	overstory	intermediate	2.01	15.5
Protium apiculatum Swart.	Burseraceae	25.8	midstory	intermediate	0.65	24.3
Coussarea paniculata (Vahl) Standl[3]	Rubiaceae	17.1	midstory	tolerant	1.48	92.5
Miconia sp.	Melastomataceae	17.2	midstory	tolerant	0.08	2.5
Amphirrhox longifolia (A.St.-Hil.) Spreng	Violaceae	5.5	understory	intermediate	0.35	908
Rinorea pubiflora (Benth.) Sprague and Sandwith	Violaceae	4.3	understory	tolerant	2.45	3104

*Species names updated since Brum *et al* . (2019).

[1] Identified in KM 67 species inventory as *Manilkara huberi* , but updated after a new floristic inventory (Herbario IAN, EMBRAPA Belem) as accepted name *Manilkara elata* .

[2] Identified in KM 67 species inventory as *Chamaecrista xinguensis* but updated after a new floristic inventory (Herbario IAN, EMBRAPA Belem) as accepted name *Chamaecrista scleroxylon* .

[3] Identified in KM 67 species inventory as *Coussarea albescens* but updated after a new floristic inventory (Herbario IAN, EMBRAPA Belem) as accepted name *Coussarea paniculata.*

List of Figures

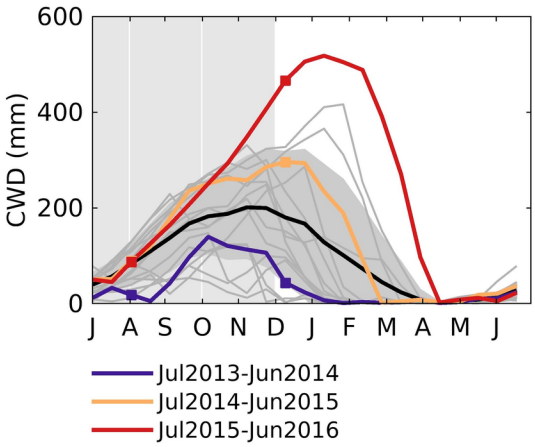

Figure 1 Monthly cumulative water deficit (mm) from 1999 to 2016 for km67 in Tapajós National Forest, Belterra-PA. NSC measurements were performed in 2013 (blue line), 2014 (orange line), and 2015 (red line). The strongest increase in CWD was observed from October 2015 to February 2016. The square dots on each blue, orange and red lines denote the months during which the NSC samples were collected. The black line and the grey shaded curve show the average monthly CWD including all years together and the ±SD around the mean. The individual grey lines show the variability of each year studied. The grey shaded square shows the period of intensification of the dry season. Details on how the CWD was computed can be found at the supplementary material.

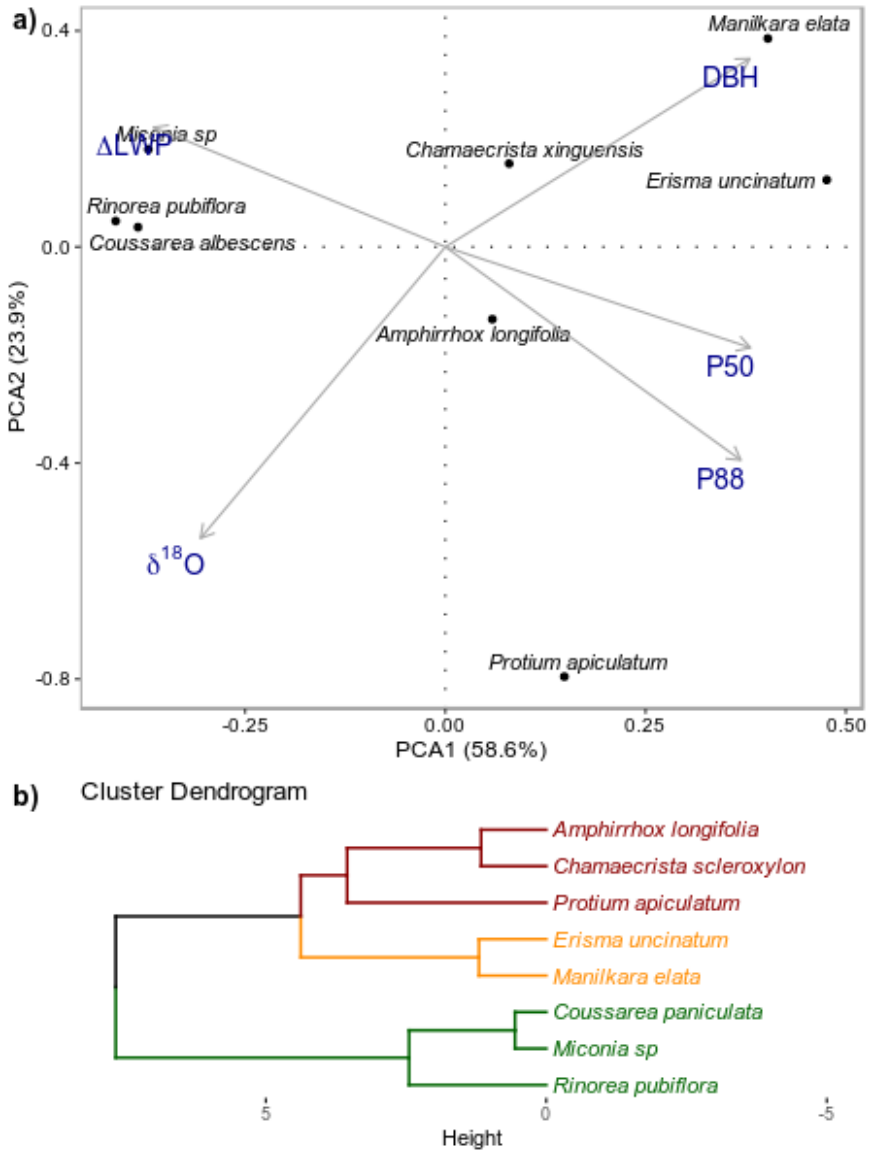

Figure 2 a) Scales of drought-resistance axis (PCA1) defined by functional hydraulic traits from eight seasonal Amazon tree species used to contrast the interannual changes of non-structural carbohydrates in leaves, branches, trunks, and roots in trees. P50 and P88 show the water potentials at which the tissue loses 50% and 88% of xylem conductance; the $\delta^{18}O$ gives the natural-abundance stable isotopes of xylem water used as proxy to determining the depths from which plants uptake soil water; the ΔLWP represents the interannual differences in the midday (12 AM - 2 PM) minimal leaf water potential measured in the field at the peak of the dry season during a non-ENSO year (December 2014) and during the ENSO drought year (December 2015); the tree DBH is the maximum diameter at breast height. We used this matrix of average values of each transformed functional hydraulic traits into a principal components analysis and obtained the PCA1. **b**) Hierarchical clustering dendrogram based on Euclidean distance showing similarities between species based on five functional hydraulic traits. We grouped species based on scaled functional hydraulic traits similarities into strategies groups: a tolerant group (green group; negative value in PCA1 axis), an intermediate group (red group, positive value in PCA1 axis close to zero and below 1) and an avoidant group

(yellow group*and* higher values in PCA1).

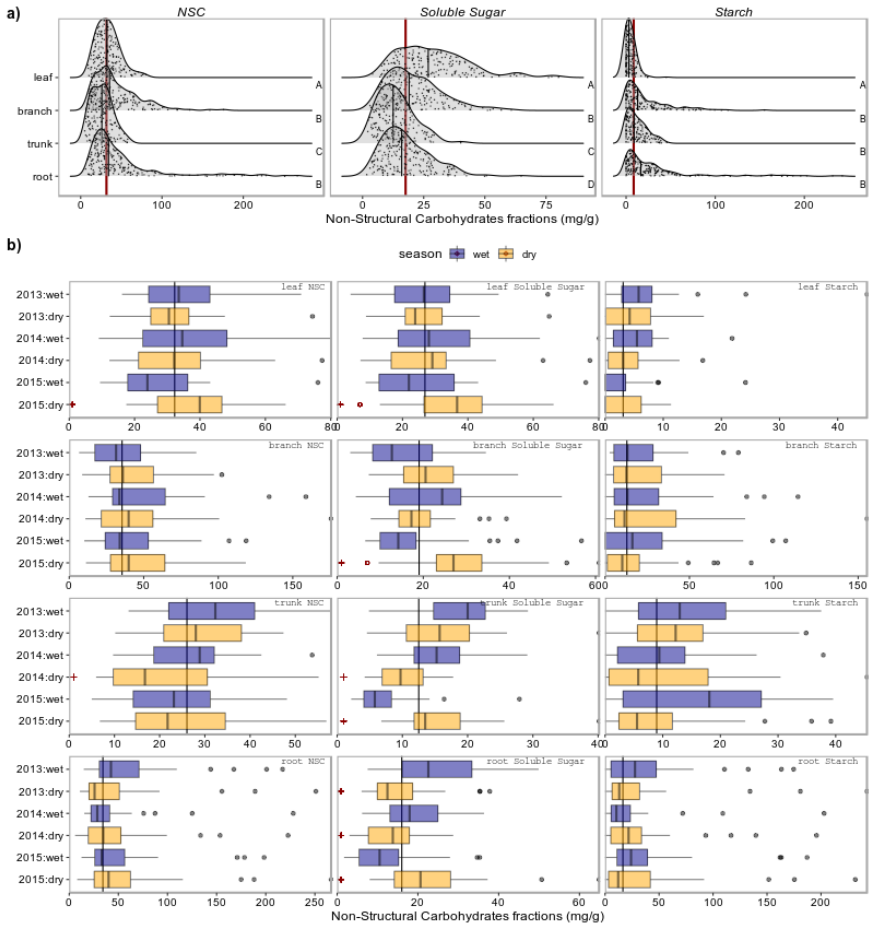

Figure 3 . **a**) Density plot of the non-structural carbohydrates (NSC) concentrations including all species together for each organ (Table 1). Each point under the curve represents one measurement, the vertical black line in each density plot shows the median values for each tree organ, and the vertical red line represents the median value for each NSC, Soluble Sugar and Starch. The upper letters in the right side represent a significant difference between average computed from PostHoc Tukey test. **b**) Box plot of the seasonal and interannual NSC concentration including all species together (Table 1). The vertical black line in each panel shows the median value of each NSC type for that organ. The symbol of a plus represents significant differences between seasons within each year. The open circle symbol represents significant differences of each specific season among years (PostHoc test; $p<0.05$). The amplitude of NSC is different between each panel because we intend to highlight the seasonal differences.

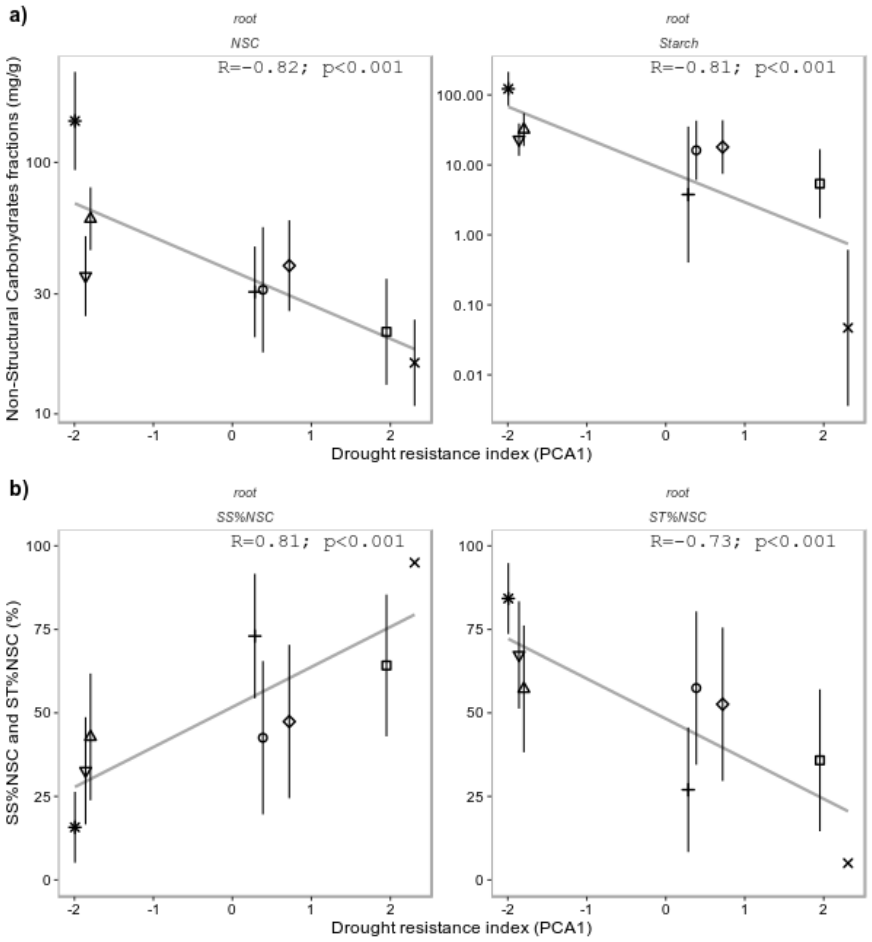

Figure 4 a) Mean (black points) and standard deviation (SD whiskers) of NSC and Starch concentration (mg g^{-1}), and **b**) the Soluble Sugar (SS) and Starch (ST) fraction of total NSC (%) of each species studied including all seasons and years together as a function of PCA1. Note that Y axis is represented in log scale. The grey line represents the linear regression line of Pearson correlation analysis. We showed only the data for starch and NSC in root because it was the unique significant relationship (see SM-Table 3). Symbols represent the species:*Manilkara elata* : square, *Erisma uncinatum* : the x symbol;*Protium apiculatum* : diamond; *Chamaecrista scleroxylon* : circle; *Amphirrhox longifolia* : cross; *Miconia sp* : triangle; *Coussarea paniculata* : inverted triangle; *Rinorea pubiflora* : asterisk.

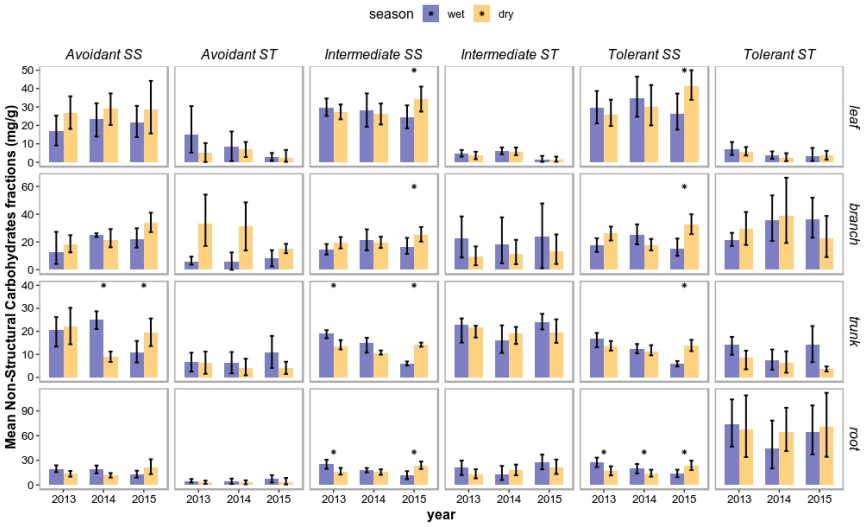

Figure 5 . Mean (columns) and confidence interval (95%, whiskers) of seasonal and interannual non-structural carbohydrates (NSC) concentration for the drought resistance groups (Table 1). The ST represents Starch, and SS represents soluble sugar. We performed the measurements at the end of the wet season (blue) and the end of the dry season (orange) during 2013, 2014, and 2015 (ENSO year). Asterisks represent differences in mean SS and ST between dry and wet seasons (PostHoc test; $p<0.05$).

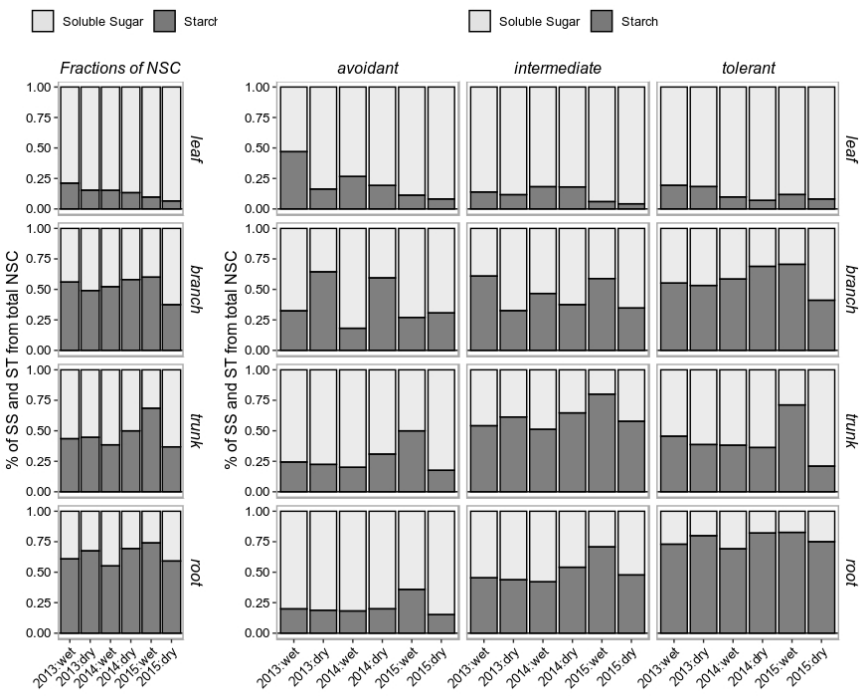

Figure 6 Fractions of soluble sugar (ligh tgrey) and starch (dark grey) with respect to total non-structural carbohydrates (NSC) in different organs and contrasting the drought-resistance groups during 2013, 2014, and 2015 grouped as wet and dry seasons.